7-1-2009

Heterologous Expression and Purification of *Vibrio proteolyticus (Aeromonas proteolytica)* Aminopeptidase: A Rapid Protocol

Mariam Hartley
Medical College of Wisconsin

Brian Bennett
Marquette University, brian.bennett@marquette.edu

Accepted version. *Protein Expression and Purification*, Vol. 66, No. 1 (July 2009): 91-101. DOI.

Heterologous expression and purification of *Vibrio proteolyticus* (*Aeromonas proteolytica*) aminopeptidase: a rapid protocol

Mariam Hartley
Department of Biophysics, Medical College of Wisconsin
Milwaukee, WI
Brian Bennett
Department of Biophysics, Medical College of Wisconsin
Milwaukee, WI

Abstract: Metalloaminopeptidases (mAPs) are enzymes that are involved in HIV infectivity, tumor growth and metastasis, angiogenesis, and bacterial infection. Investigation of structure-function relationships in mAPs is a prerequisite to rational design of anti-mAP chemotherapeutics. The most intensively studied member of the biomedically important dinuclear mAPs is the prototypical secreted *Vibrio proteolyticus* di-zinc aminopeptidase (VpAP). The wild-type enzyme is readily purified from the supernatant of cultures of *V. proteolyticus*, but recombinant variants require expression in *Escherichia coli*. A greatly improved system for the purification of recombinant VpAP is described. A VpAP-$(His)_6$ polypeptide, containing an N-terminal propeptide, and a C-terminal $(His)_6$ adduct, was purified by metal ion affinity chromatography from the supernatant of cultures of *E. coli*. This single step replaced the sequence of $(NH_4)_2SO_4$ fractionation, and anion exchange and hydrophobic interaction chromatographic separations of earlier methods. Traditionally, recombinant VpAP proenzyme has been treated with proteinase K and with heat (70 °C), to remove the N- and C-terminal regions, and yield the mature active enzyme. This method is unsuitable for VpAP variants that are unstable towards these treatments. In the new method, the hitherto

Protein Expression and Purification, Vol. 66, No. 1 (July 2009): pg. 91-101. DOI.

noted, but not fully appreciated, ability of VpAP to autocatalyze the hydrolysis of the N-terminal propeptide and C-terminal regions was exploited; extensive dialysis of the highly purified VpAP-$(His)_6$ full-length polypeptide yielded the mature active protein without recourse to proteinase K or heat treatment. Purification of variants that have previously defied isolation as mature forms of the protein was thus carried out.

Introductory Statement

Metalloaminopeptidases (mAPs) are key players in many biological processes, including cellular targeting of proteins [1, 2], protein degradation [1, 3, 4], aging [5-10], tissue repair [11-15], cataract formation [16-22], HIV infectivity [23-26], angiogenesis [27-31], and carcinogenesis [27, 32-34]. A biomedically important family of mAPs is that of the dinuclear mAPs, also known as "cocatalytic" mAPs [35]. The dinuclear mAPs hydrolyze the N-terminal amino acid from peptides and proteins, with varying degrees of substrate specificity, and are characterized by an active site that contains two transition ions, usually Zn(II), separated by about 0.35 nm (3.5 Å) in a dinuclear active site. The most intensively studied and well characterized of these enzymes is the 32kD secreted di-zinc leucine aminopeptidase, VpAP, from *Vibrio proteolyticus* (formerly *Aeromonas proteolytica*) [36-40]. It appears that one of the metal ions in VpAP and related mAPs is involved in nucleophile activation, and is essential for catalysis, whereas the other is involved in substrate activation and stabilization of the transition state [36, 39, 41]; the non-essential metal ion may thus be key to substrate specificity, though conclusive evidence is lacking. Other dinuclear mAPs that have been studied include the angiogenesis target methionyl aminopeptidase, and the secreted aminopeptidases that are virulence factors in the pathogenicity of certain species of *Clostridium, Streptomyces, Vibrio* and *Aeromonas* [42-48]. VpAP itself exhibits a very high degree of structural homology with the protease domain of the prostate-specific membrane antigen (PSMA) [49]. PSMA is highly expressed in prostate cancer cells [50], but its role in prostate cancer is currently unknown. Some potent inhibitors of VpAP and its homologs, including bestatin (ubenimex), ovalicin, and fumagillin, have also been shown to exhibit *in vivo* activity against tumor growth, angiogenesis, and HIV infectivity [8, 24, 51-59]. Wild-type VpAP is readily available in large quantities from *V. proteolyticus*, and it is an excellent model protein with which to explore the structure-function relationships of mAPs: studies on

Protein Expression and Purification, Vol. 66, No. 1 (July 2009): pg. 91-101. DOI.

VpAP have provided information that may lead to the design of more effective and specific chemotherapeutic agents [35, 39-41, 60]. However, recent work on VpAP and VpAP homologs has shown that site-directed recombinant variants can provide important mechanistic information that is unavailable with the native proteins [61-64]. A need exists, therefore, for an efficient expression system and purification protocol for recombinant VpAP that can provide sufficient quantity of high-purity material for physicochemical, structural, and spectroscopic study of site-directed variants of VpAP.

VpAP has been isolated from cultures of *V. proteolyticus* since the mid-1960s. Investigation of the proteolytic activity associated with *V. proteolyticus* [65] led to the identification and isolation of VpAP by Prescott and Wilkes [66]. Subsequent refinements of the purification procedure [67, 68] resulted in a protocol that yielded VpAP preparations that were sufficiently homogenous for crystallization. The purification of VpAP is complicated by the fact that the 32 kDa mature active protein is the product of substantial processing of a 54 kDa translated polypeptide, VpAP*, coded for by the native ORF [69, 70]. The 54 kDa VpAP* polypeptide consists of a 21 amino acid signal peptide, an 85 amino acid N-terminal propeptide, a 299 amino acid mature region, and a 99 amino acid C-terminal propeptide (Figure 1). The signal peptide is required for secretion, the N-terminal propeptide is required for folding but its presence inhibits catalytic activity, and the C-terminal propeptide is of undetermined function but appears to be species-specific [71, 72]. VpAP* is processed to the final 32 kDa mature protein only after secretion and during purification; roles in the processing of VpAP* have been proposed for VpAP* itself (and VpAP) in autoprocessing, for a co-expressed neutral protease, and for a heat-treatment step that has been traditionally employed [73-75]. An additional problem in the purification of VpAP for spectroscopic studies is the presence of two low M_r (< 2kD) brown pigments, one of which contains spectroscopically active Fe(III), that appear to be closely associated with VpAP; any successful protocol must separate these pigments from VpAP [76].

Protein Expression and Purification, Vol. 66, No. 1 (July 2009): pg. 91-101. DOI.

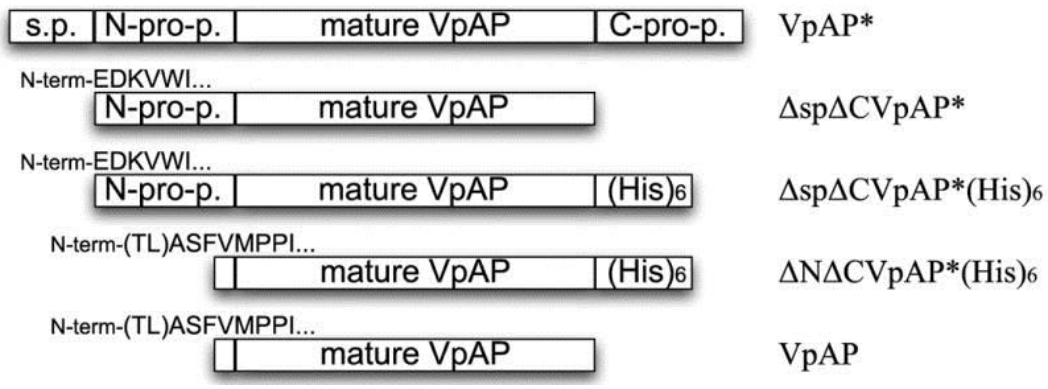

Figure 1. Linear representations of various VpAP species. VpAP* is the native polypeptide secreted by *V. proteolyticus*. ΔspΔCVpAP* is the polypeptide secreted by *E. coli* expressing a construct of VpAP lacking the C-terminal polypeptide. ΔspΔCVpAP*$(His)_6$ is the polypeptide secreted by *E. coli* containing a plasmid that included the new construct described herein. N-terminal processing of ΔspΔCVpAP*$(His)_6$ yields ΔNΔCVpAP*$(His)_6$, and subsequent C-terminal processing yields the mature VpAP polypeptide. The experimentally observed N-terminal sequences are shown. The N-terminal sequence of natively expressed mature VpAP is MPPI. Proteinase K treatment of recombinant VpAP* yielded a final N-terminal sequence of ASFVMPPI, whereas autoprocessing resulted in an N-terminal sequence of TLASFVMPPI. "N-pro-p." and "C-pro-p." denote the N- and C-terminal propeptides, respectively, and "s.p." denotes a signal peptide.

The commonly and successfully used protocol for the purification of VpAP from *V. proteolyticus* involves (i) rapid separation of the supernatant from *V. proteolyticus* cells; (ii) $(NH_4)_2SO_4$ fractionation of the supernatant; (iii) heat treatment (70 °C for 5 – 7 h), followed by dialysis and clarification by centrifugation and filtration (0.22 μm); (iv) one or two hydrophobic interaction chromatographic fractionations (octyl-Sepharose); and (v) anion-exchange chromatography (Q-Sepharose). A highly detailed investigation into the requirements for the isolation of VpAP heterologously expressed in *E. coli* has been described by Bzymek, Holz and coworkers [71], and the resulting protocol has yielded both recombinant wild-type and site-directed variant forms of VpAP for subsequent crystallographic and physicochemical studies [38, 61-63, 71]. As suggested by earlier work [72, 77-79], it was found that VpAP was best expressed as a 52 kDa proenzyme (ΔspVpAP*; lacking the first 23 amino acids); the use of an appropriate leader sequence (*e.g.* the pelB sequence of pET26b(+)) results in secretion of the proenzyme, which can be purified from the supernatant. Essentially the same purification procedure as for the native enzyme from *V. proteolyticus* was adopted, except for an additional incubation with proteinase K (PK), which appears to mimic

the effects of *V. proteolyticus* neutral protease and removes the N-terminal propeptide, prior to heat treatment.

In the course of our own studies, we have followed the earlier procedure [71] for the purification of recombinant wild-type and variant VpAP and have successfully isolated VpAP with amino acid substitutions in the active site pocket and in an adjacent hydrophobic pocket [39]. However, we have also encountered problems, including (i) irreproducible, and generally low, yields of VpAP; (ii) unpredictability of the effects of PK on variant forms of VpAP*; and (iii) the inability to isolate some site-directed variants as the mature proteins, notably variants with substitutions of Asp99. In the present work, we describe a rapid purification scheme for heterologously expressed VpAP that reproducibly yields 10 mg of pure wild-type VpAP per liter of *E. coli* culture. In addition, we describe the expression and purification of the D99A, D99H, and D99M variant forms of VpAP, that had hitherto defied isolation as mature proteins. The advantages of the new method are discussed.

Materials and Methods

General chemicals and reagents

Restriction enzymes, T4 DNA ligase, and Antarctic phosphatase were purchased from New England Biolabs (Ipswich, MA). A dNTP cocktail and Pfu Turbo polymerase were purchased from Stratagene (La Jolla, CA). BL21 Star DE3 One Shot Chemically Competent *E. coli* cells were purchased from Invitrogen (Carlsbad, CA). LB medium and kanamycin were purchased from Fisher Scientific (Fair Lawn, NJ). IPTG was obtained from Anatrace Incorporated (Maumee, OH), aliquoted into 1 ml volumes of 1 M concentration, and stored at −20 °C until use. Pre-cast PAGE gels were purchased from BioRad Laboratories (Hercules, CA). Agarose bead-linked proteinase K from *Tritirachium album* was purchased from Sigma-Aldrich (St. Louis, MO). All other general chemicals (ACS grade) and buffer salts (Biotech or electrophoresis grade) were obtained from Sigma-Aldrich (St. Louis, MO). Deionized water was additionally filtered for organic and metal ion contaminants using a Milli-Q system (Millipore, Molsheim, France) and exhibited a resistance of > 18 MΩ.

Protein Expression and Purification, Vol. 66, No. 1 (July 2009): pg. 91-101. DOI.

Plasmids

cDNA was amplified by PCR from the plasmid pVSNMC [72], obtained from the Applied Enzymology Laboratory of the National Food Research Institute (Ibaraki, Japan), using the forward and reverse primers 5′-GGCTTCCATGGAAGACAAAGTGTGGATCTCA-3′ (forward; NcoI site underlined), and 5′-GCGCGCCTCGAGCTGATTGCC-3′ (reverse; XhoI site underlined). The PCR product was then inserted between the NcoI and XhoI sites of pET26b(+) (Invitrogen, Carlsbad, CA). The reverse primer lacked the VpAP native stop codon, thus transcription continued through the $(His)_6$-coding sequence immediately downstream of the XhoI site in pET26b(+), and was stopped immediately after $(His)_6$. The resulting construct, pAPMH, was used to express a wild-type polypeptide (ΔspΔCVpAP*$(His)_6$) containing the N-terminal propeptide, the mature VpAP polypeptide, and a C-terminal $(His)_6$ construct, but lacking the signal sequence and the C-terminal propeptide. pAPMH was also used as the template to generate VpAP site-directed variants.

Recombinant DNA for the D99A, D99M, and D99H variants of VpAP was generated using the following primers (mutations underlined):

D99A forward, 5′-GGTGGTCACCTTGCTTCGACCATTGGTTCAC-3′;
D99A reverse, 5′-GAACCAATGGTCGAAGCAAGGTGACCACC-3′;
D99M forward, 5′-GGTGGTCACCTTATGTCGACCATTGGTTCACAC-3′;
D99M reverse, 5′-GTGTGAACCAATGGTCGACATAAGGTGACCACC-3′;
D99H forward, 5′-GGTGGTCACCTTCATTCGACCATTGGTTCACAC-3′;
D99H reverse, 5′-GGTGGTCACCTTCATTCGACCATTGGTTCACAC-3′.

A six-step PCR protocol was employed with the following parameters: *step 1*, 95 °C for 1 min; *step 2*, 95 °C for 30 s; *step 3*, primer T_m – 10 °C, 1 min; *step 4*, 68 °C for 8 min; *step 5*, 18 cycles of steps 2 – 4; *step 6*, 68 °C for 10 min.

All constructs were fully sequenced (Applied Biosystems ABI PRISM 3100 analyzer, Protein and Nucleic Acid Facility, Medical College of Wisconsin, Milwaukee, WI) and found to contain no mutations except for those intended. Sequence-verified constructs were used to transform BL21 Star (DE3) One Shot Chemically Competent *E. coli* cells (F- *omp*T *hsd*SB (*r*B-mB-) *gal dcm rne1*31 (DE3)), using the

transformation protocol provided by the manufacturer (Invitrogen, Carlsbad, CA). Frozen stocks were prepared by adding 1 ml bacterial culture ($OD_{600\ nm} \approx 0.6$) to 1 ml 30% glycerol (in water), snap frozen in liquid nitrogen, and stored at −80 °C.

Expression of VpAP

Starter cultures were prepared by inoculation of 20 ml LB, containing 30 μg/ml kanamycin, with a scraping from frozen stock cultures, followed by agitation at 250 rpm, 37 °C, in a 50 ml conical tube, until the $OD_{600\ nm}$ reached 1.0. Cultures for VpAP expression were prepared by adding 2.5 ml of starter culture to a 1 L flask containing 250 ml LB (30 μg/ml kanamycin). Flasks were agitated in an orbital shaker at 250 rpm, 37 °C until $OD_{600\ nm} = 0.6$. IPTG was added (to a final concentration of 1 mM), and flasks were further agitated for 18 h, 250 rpm, 30 °C.

Assay of VpAP

Steady state VpAP activity was estimated from spectrophotometric determination of the rate of formation of the product, *p*-nitroaniline (PNA), of hydrolysis of L-leucine-*p*-nitroaniline (LPNA; Sigma, St. Louis, MO), at 405 nm, 25 °C. The assay mixture contained 1.0 mM LPNA in 10 mM Tricine buffer, pH 8.0 [67, 80] and a differential extinction coefficient $\Delta\varepsilon_{405\ nm} = 10{,}800\ M^{-1}\ cm^{-1}$ was employed [81]. A "Unit" of activity was defined as a rate of hydrolysis of 1 μmol LPNA min^{-1} under these conditions. Apparent kinetic parameters K'_m and k'_{cat} were estimated by collecting the entire progress curve, with initial [LPNA] = 0.1 mM, and fitting the part of the curve that exhibited a linear relationship between $t^{-1}[\ln([S_0]/[S_t])]$ and $t^{-1}[S_0 - S_t]$ [39, 82]. This approach indicated that the steady state assay routinely underestimated V_{max} by a factor of 1.3, likely because of weak substrate inhibition, but steady state values were determined for wild-type VpAP for comparison to other studies. Quantities of ΔspΔCVpAP*$(His)_6$ were estimated spectrophotometrically, taking $\varepsilon_{280\ nm} = 58{,}110\ M^{-1}\ cm^{-1}$, and purified mature VpAP protein was estimated taking $\varepsilon_{280\ nm} = 43{,}950\ M^{-1}\ cm^{-1}$ [76, 83-85]. SDS-PAGE analysis was carried out on precast 4 - 15 % polyacrylamide/Tris-HCl gels (BioRad "Ready Gels"). Samples of VpAP were generally loaded directly onto

SDS-PAGE gels without pretreatment. Occasionally, samples were heated for 5 min at 95 °C in the presence of either 33 mM dithiothreitol, 66 mM β-mercaptoethanol, or both, prior to SDS-PAGE analysis. These pretreatments were found to diminish the intensities of bands showing anomalously high apparent M_r, but did not affect the number or the positions of the bands. SDS-PAGE analyses presented herein were carried out on samples that had not been pretreated, except where explicitly stated in the figure legend (*i.e.* only Figure 4).

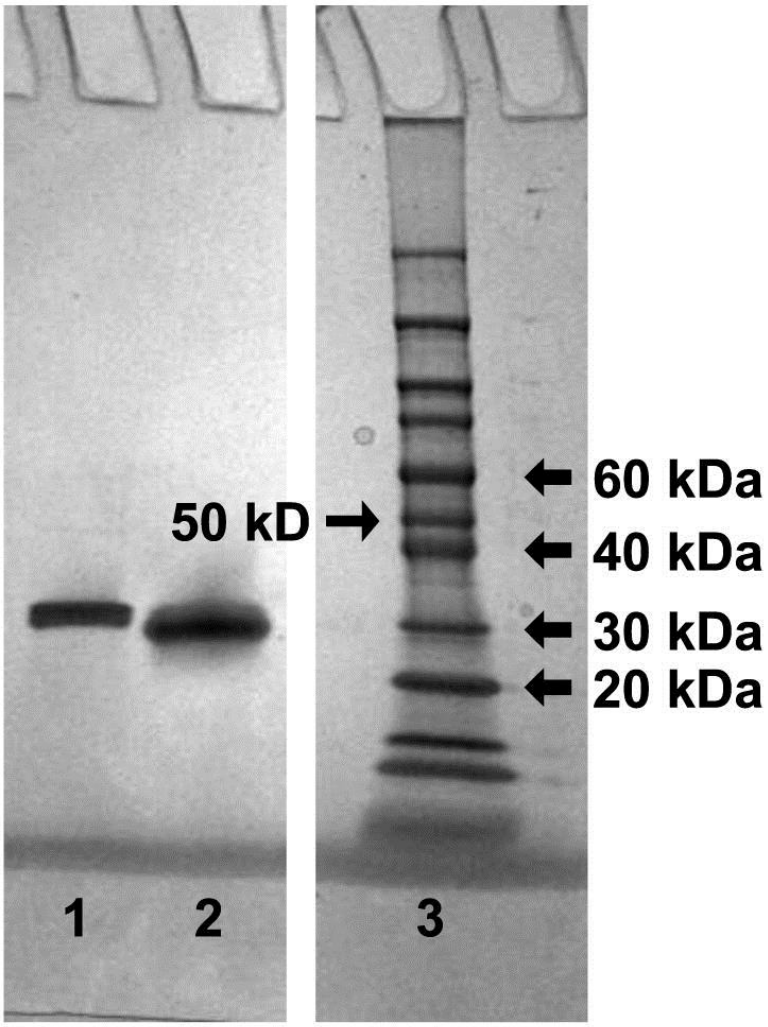

Figure 4: Time dependence of incubation with proteinase K on the apparent M_r of VpAP. Lane 1, Recombinant VpAP prior to proteinase K exposure; Lane 2, after further incubation (90 min) with proteinase K; Lane 3, M_r markers. (β-mercaptoethanol and dithiothreitol were employed in the sample buffers).

Protein Expression and Purification, Vol. 66, No. 1 (July 2009): pg. 91-101. DOI.

Purification of wild-type VpAP

Step A: Cultures were clarified by centrifugation (5200 × *g*, 10 min, 4 °C), and 1 L supernatant was applied (3.0 ml/min, 4 °C) to 15 ml TALON Superflow Metal Affinity Resin (Clontech, Mountain View, CA). The resin was washed with 75 ml of 50 mM HEPES buffer, pH 7.5, at 1.0 ml/min. HEPES buffer (50 mM, pH 7.5), containing imidazole (20 mM), was applied (3.0 ml/min) to effect protein elution. Fractions (6 ml) were assayed for activity and protein content. In order to speed future identification of fractions containing site-directed variants of VpAP that may show no detectable activity, the retention volumes for the fractions of wild-type VpAP with highest specific activity were characterized from the commencement of application of imidazole. Fractions containing protein and expressing VpAP activity were combined and dialyzed at 4 °C against 50 mM HEPES buffer, pH 7.5, to dilute imidazole to a final concentration of < 1 nM.

Step B: The dialysate from Step A was agitated (250 rpm, 37 °C) with ≈ 5 mg (≈ 0.025 units; ≈ 1 μg protein equivalent) PK agarose beads. Aliquots were periodically assayed for VpAP activity toward LPNA. When the activity toward LPNA ceased to increase upon further incubation with PK (generally ≈ 40 min), the VpAP-containing suspension was filtered to remove the PK beads (0.22 μm, Millipore mixed cellulose esters [MCE] syringe filter).

Step C: The solution from Step B was immediately incubated at 70 °C in a water bath, either until the activity began to decrease, or else for 1 h. The suspension was cooled on ice, filtered (0.22 μm), and dialyzed (50 mM HEPES, pH 7.5, 4 °C).

Step D: The solution from Step C was applied (2.0 ml/min, 4 °C) to a 15 ml TALON Co(II)-affinity resin column. HEPES buffer (50 mM, pH 7.5) was applied, and eluate fractions that contained the highest specific activity toward LPNA were pooled and concentrated by ultrafiltration (Amicon PM10). As in Step A, retention volumes were characterized.

Protein Expression and Purification, Vol. 66, No. 1 (July 2009): pg. 91-101. DOI.

Purification of VpAP D99-substituted variants D99A, D99H and D99M

Step A was carried out as for wild-type VpAP. Because the activities of the D99-substituted variants were extremely low at this stage, fractions were collected using the retention volumes characterized for wild-type. Protein content was estimated from $A_{280\ nm}$. Steps B and C, however, were replaced by *Step E*, which entailed extended (7 – 14 d) dialysis against HEPES buffer (50 mM, pH 7.5) at 4 °C. Self-processing of VpAP D99-substituted variants was monitored by SDS-PAGE on 4 – 20 % polyacrylamide gradient gels. When SDS-PAGE and N-terminal amino acid sequencing indicated complete processing, the dialysate was filtered (0.22 μm), and further processed as described for Step D for wild-type VpAP. The previously characterized retention volumes for wild-type VpAP were used as an aid to identifying fractions containing VpAP D99-substituted variants.

N-terminal amino acid sequencing

Proteins were separated on SDS-PAGE gels, transferred to polyvinylidene fluoride membranes, excised, and N-terminal sequenced by Edman degradation using a Beckman Porton LF3000G sequencer with in-line Applied Biosystems PTH analyzer, at the Protein and Nucleic Acid Core Facility at the Medical College of Wisconsin.

Circular dichroism spectropolarimetry

Circular dichroism spectra were recorded at 25 °C using a JASCO J-710 spectropolarimeter equipped with a 1 mm path-length quartz cell. Samples for spectropolarimetry were equilibrated with 5 mM phosphate buffer, pH 7.5, by dialysis.

Crystallization of heterologously expressed VpAP

VpAP was crystallized from a hanging drop. VpAP (0.5 mM) in 10 mM Tris buffer, pH 8.0, containing 10 mM KSCN and 400 mM NaCl was equilibrated with 100 mM Tris buffer, pH 8.0, containing 100 mM KSCN and 4.5 M NaCl, at 19 °C.

Protein Expression and Purification, Vol. 66, No. 1 (July 2009): pg. 91-101. DOI.

X-ray diffraction

Diffraction data were collected on a single crystal of heterologously expressed wild-type VpAP, with Paratone-N (Hampton) as a cryoprotectant, at −160 °C on a Rigaku R-AXIS IV++ diffractometer using Crystal Clear software [86]. An oscillation step size of 1.0° was used to collect 3 min exposures. Data were processed and unit cell parameters determined with HKL2000 [87]. Phases were derived from a structure previously solved in this laboratory (accession code 2IQ6 [88]) and used to solve the structure by molecular replacement using Phaser [89]. Model building was performed with the graphic program COOT [90]. The structure was manually inspected with electron density maps and with $2F_{obs} - F_{calc}$ and $F_{obs} - F_{calc}$ coefficients. Structures were refined using iterative cycles of energy minimization using REFMAC5 [91] in the CCP4 program suite [92], alternating with manual map-fitting and model rebuilding. Progress of the refinement was confirmed by the steady decrease in both the $R_{crystal}$ and R_{free} values. Procheck was used to check Ramachandran (φ, ψ) values [93].

Results

Expression and purification of wild-type VpAP

10 L of *E. coli* culture, $OD_{600\ nm}$ = 2.3, yielded 20 g wet weight of cells, which were discarded. Up to 10 mg of wild-type VpAP, with a steady state ([LPNA] ≈ 1 mM) specific activity of 120 Units/mg at 25 °C, was purified from the supernatant. The purification of wild-type VpAP is summarized in Table 1. Kinetic analysis indicated apparent Michaelis-Menten parameters k'_{cat} = 82 ± 2 s^{-1}, and K'_m = 18 ± 1 μM.

Table 1: Purification of wild-type VpAP

Purification step	Volume (ml)	Total protein (mg)	Activity (Units)	Specific activity (Units/mg)
Supernatant clarification	10,000	120,000[a]	320	0.003[a]
Step A	20	80	480	6
Steps B and C	20	68	7480	110
Step D	40	60	7200	120

[a]VpAP was purified from the supernatant of bacterial cultures grown in LB medium, that originally contained about 12 g/L of a mixture of peptides, peptones and proteins.

Protein Expression and Purification, Vol. 66, No. 1 (July 2009): pg. 91-101. DOI.

Step A: VpAP-containing fractions that eluted during Co(II)-affinity chromatography upon the application of imidazole were characterized by three bands on SDS-PAGE, at apparent M_r ≈ 57 kDa, ≈ 42 kDa, and ≈ 32 kDa (bands A, B, and C of Figure 2). The relative intensities of the bands appeared to be the same for each fraction. The origin of the the "57 kDa" band, A, is unclear, as the cDNA coded for the 42kD ΔspΔCVpAP*$(His)_6$ polypeptide, but that material evidently bound the Co(II) affinity resin with an affinity comparable to that for the material responsible for the other two bands. N-terminal amino acid sequencing of the other two bands, B and C, indicated the same N-terminal sequence of EDKVWI for each, corresponding to the N-terminal region of the 85 amino acid N-terminal propeptide, and these bands were only observed in fractions that eluted upon the application of imidazole, so contain the $(His)_6$ adduct. Despite the apparent M_rs from SDS-PAGE, then, both bands B and C must be due to ΔspΔCVpAP*$(His)_6$. The specific activity of the material following Step A was ≈ 6 Units/mg, consistent with the retention of the inhibitory N-terminal propeptide in > 95 % of the polypeptide molecules.

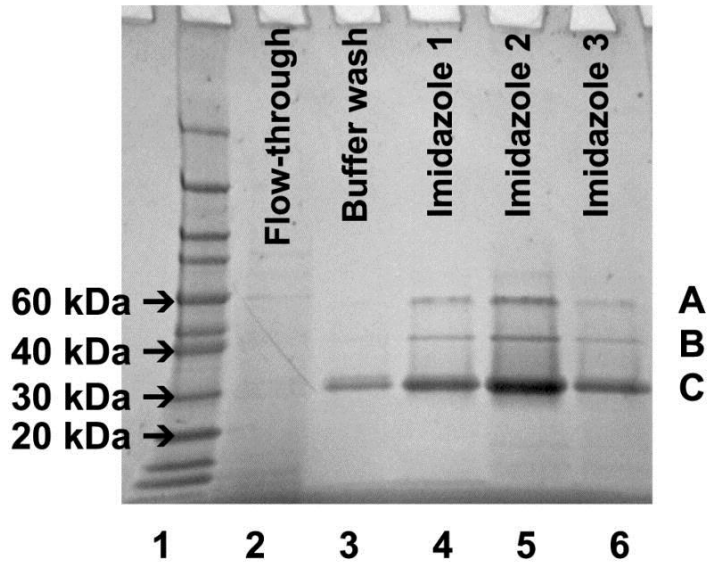

Figure 2: SDS-PAGE analysis of Co(II)-affinity resin chromatographic fractionation of wild-type VpAP-induced *E. coli* culture supernatant. Lane 1, M_r markers (pre-stained Novex Sharp, Invitrogen; note that the band between 40 kDa and 60 kDa is 50 kDa); Lane 2, Flow-through during application of supernatant; Lane 3, Flow-through during washing with HEPES buffer; Lanes 4 - 6, Eluate upon application of imidazole-containing buffer.

The anomalous behavior of VpAP on SDS-PAGE is worthy of comment. The apparent M_r of proteins from SDS-PAGE can be very sensitive to even very minor differences in physicochemical properties of polypeptides in some cases [94, 95]. Here, the origin of the anomalous behavior on SDS-PAGE is unknown, but may be related to the presence of cysteines with the potential to form disulfide bonds. Mature VpAP contains only two cysteines, Cys223 and Cys227, that form a disulfide bond. Larger recombinant constructs, however, contain up to three additional cysteines; one is in the N-terminal propeptide, and two reside in the C-terminal propeptide. The ΔspΔCVpAP*$(His)_6$ construct contains three cysteines. It is highly likely, given the thermostability of VpAP, that the Cys223-Cys227 disulfide bond is very stable and that neither of these cysteines forms a disulfide bond with the third cysteine in any significant fraction of the sample. It is, however, possible that the cysteine that resides on the N-terminal propeptide engages in intermolecular disulfide bond formation. The presence of the N-terminal propeptide inhibits activity and so likely is adjacent to the active site in the folded polypeptide; given the extensive secondary structure and hydrophobic surface of VpAP, dimers thus formed would likely be of high stability and possibly partially resistant to SDS, leading to incomplete unfolding and the presence of multiple bands. In SDS-PAGE analysis of VpAP after Step A, pretreatment of samples by heating with β-mercaptoethanol and/or dithiothreitol was found to diminish the intensity of the "57 kDa" and "42 kDa" bands somewhat, but not completely. The thermostability of VpAP (see Step C) may be related to this phenomenon. An additional factor that may contribute to the anomalous behavior of unprocessed and partially processed VpAP on SDS-PAGE is the presence of regions of high hydrophobicity in both the mature VpAP sequence [96], and, particularly, in the N-terminal propeptide.

Steps B and C: SDS-PAGE comparison of the material from Step A (Lane 2, Figure 3) with those from Steps B (Lane 3, Figure 3) and C (Lane 4, Figure 3) shows clear differences. Treatment with PK yielded a dominant species with an apparent M_r of 32 kDa, and some minor species of higher and lower apparent M_r. In contrast to results from Step A, N-terminal sequencing of the major band from Step B returned ASFVMP, indicating loss of the N-terminal propeptide [71]; the N-terminal region of mature natively-expressed VpAP begins MPPI, and is preceded in this recombinant protein by ASFV from the C-terminal

sequence of the N-terminal propeptide. The specific activity of ≈ 110 Units/mg was consistent with removal of the N-terminal propeptide. More extensive incubation with PK (> 1 h) yielded a species with an apparent M_r of 28 kDa, with no change in catalytic activity (Figure 4). Two bands with apparent M_r of 28 and 32 kDa are routinely observed with preparations of natively-expressed VpAP, and mass spectrometry has indicated that the two bands correspond to species with almost indistinguishable M_rs of 32 ± 1 and 31 ± 1 kDa [71]. Further processing of PK-treated VpAP by heat treatment (*i.e.* Step C) yielded a single species that was indistinguishable on SDS-PAGE (Lane 4, Figure 3) or by Co(II)-affinity resin binding behavior (Figure 5) from the major species observed prior to heat treatment; heat treatment served to denature fragments that had been cleaved upon PK treatment. In addition, following Step C, it was observed that the VpAP activity could be recovered from Co(II)-affinity resin with HEPES buffer, in the *absence* of imidazole, indicating that the C-terminal $(His)_6$ region was no longer present following Steps B and C. The specific activity of 120 Units/mg for VpAP from Step C does not, in fact, indicate any enhancement of the activity per mole upon heat treatment, but reflects the removal of the cleaved N-terminal propeptide, about 60 % of which appeared to have denatured during PK-treatment and dialysis, and was removed by centrifugation, and the remainder of which was denatured by heat treatment.

Protein Expression and Purification, Vol. 66, No. 1 (July 2009): pg. 91-101. DOI.

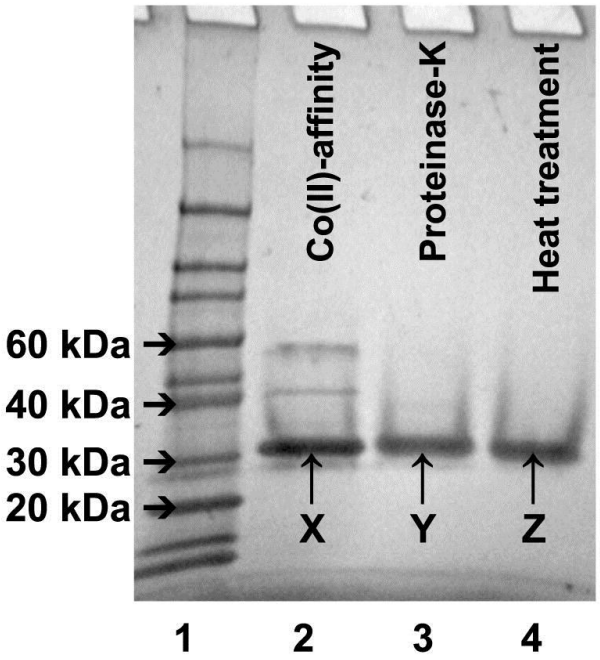

Figure 3: Effects on SDS-PAGE analysis and N-terminal sequence of incubation with proteinase K and heat treatment on Co(II)-afinity resin-fractionated wild-type ΔspΔCVpAP*(His)$_6$. Lane 1, M_r markers; Lane 2, Co(II)-afinity resin-fractionated ΔspΔCVpAP*(His)$_6$; Lane 3, ΔspΔCVpAP*(His)$_6$ fraction (Lane 2) incubated with proteinase K until maximum activity was reached; Lane 4, subsequent heat treatment of material from Lane 3. Band X (Lane 2) returned an N-terminal sequence EDKVWI; Bands Y and Z (Lanes 3 and 4, respectively) returned ASFVMP.

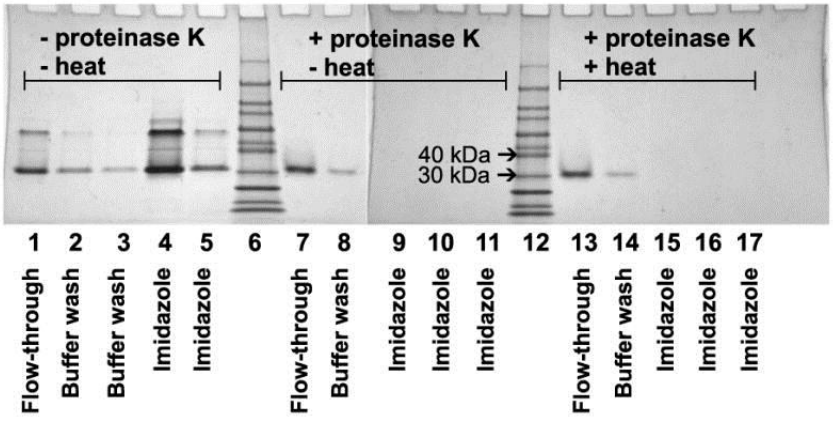

Figure 5: Fractionation of VpAP at various stages of processing by Co(II)-affinity resin. Wild-type ΔspΔCVpAP*(His)$_6$ obtained by Co(II)-affinity resin fractionation was re-applied to Co(II)-affinity resin without further treatment (Lanes 1 - 5), after incubation with proteinase K (Lanes 7 - 11), and after proteinase K and heat treatment (Lanes 13 - 17). Fractions were collected during application of the sample ("Flow-through", Lanes 1, 7 and 13), during washing with HEPES buffer (Lanes 2, 3, 8 and 14), and upon application of imidazole-containing buffer (Lanes 4, 5, 9 - 11 and 15 - 17), and analyzed by SDS-PAGE. M_r markers are shown in Lanes 6 and 12.

Protein Expression and Purification, Vol. 66, No. 1 (July 2009): pg. 91-101. DOI.

Step D: The purpose of Step D was to separate any VpAP that had not had the C-terminal $(His)_6$ removed during Step B and had yet remained undenatured during Steps B and C. SDS-PAGE analyses (Figure 5) indicated that no detectable amount of protein eluted from the Co(II)-affinity resin upon the application of imidazole.

Expression and purification of VpAP:D99X variants

10 L *E. coli* cultures, $OD_{600\ nm}$ = 2.0 - 2.3, yielded 15 - 20 g wet weight of cells, which were discarded. From 1 to 2.5 mg of the D99-substituted variants of VpAP were purified from the supernatants. Steady state activities towards LPNA were significantly lower than for wild-type VpAP: the activities of VpAP:D99M, VpAP:D99H and VpAP:D99A were 0.030 ± 0.002, 0.004 ± 0.001, and 1.5×10^{-4} to 3.5×10^{-4} Units/mg, respectively. The purification of VpAP:D99M is summarized in Table 2. Apparent kinetic parameters of k'_{cat} = 1.0 ± 0.1 min^{-1}, and K'_m = 31 ± 7 μM were estimated from kinetic analysis of VpAP:D99M; meaningful values for K'_m could not be obtained for the other variants due to the very low activities.

Table 2: Purification of VpAP:D99M

Purification step	Volume (ml)	Total protein (mg)	Activity (Units)	Specific activity (Units/mg)
Supernatant clarification	10,000	120,000[a]	N.D.[b]	N.D.[b]
Step A	20	3	N.D.[b]	N.D.[b]
Step B[c]	20	N.D.[b]	N.D.[b]	N.D.[b]
Step E[c]	20	2.4	0.07	0.03
Step D[d]	60	2	0.06	0.03

[a]VpAP was purified from the supernatant of bacterial cultures grown in LB medium, that originally contained about 12 g/L of a mixture of peptides, peptones and proteins.
[b]"N.D." signifies none detected.
[c]Step B and Step E are alternative procedures; either Step B or Step E was carried out, not both.
[d]Step D was carried out only on material from Step E, not from Step B.

Step A processing of supernatant containing ΔspΔCVpAP:D99*X**$(His)_6$, where *X* = A, H or M, proceeded as for wild-type VpAP, except that no activity towards LNPA was detectable at that stage. In addition, the apparent M_r of the bands that eluted from the Co(II)-affinity resin upon application of imidazole differed slightly from wild-type (SDS-PAGE of crude VpAP:D99A after Step A is shown as lane 4 of Figure 6 and crude VpAP:D99M is shown as Lane 1 of

Figure 7; compare with wild-type VpAP, lane 5, Figure 2). The differences between the non-reducing SDS-PAGE profiles of wild type VpAP and of the VpAP:D99*X* variants may be related to the cysteine content, just as the cysteine content may be responsible for the presence of multiple bands, some with M_r higher than the molecular species present, in the first place. In wild-type VpAP, the Cys223-Cys227 disulfide bond is very stable, as attested to by the thermostability of VpAP. Asp99 is a key residue in a hydrogen bonding network that involves active site residues; indeed, it is of interest because of its possible structural and catalytic roles.

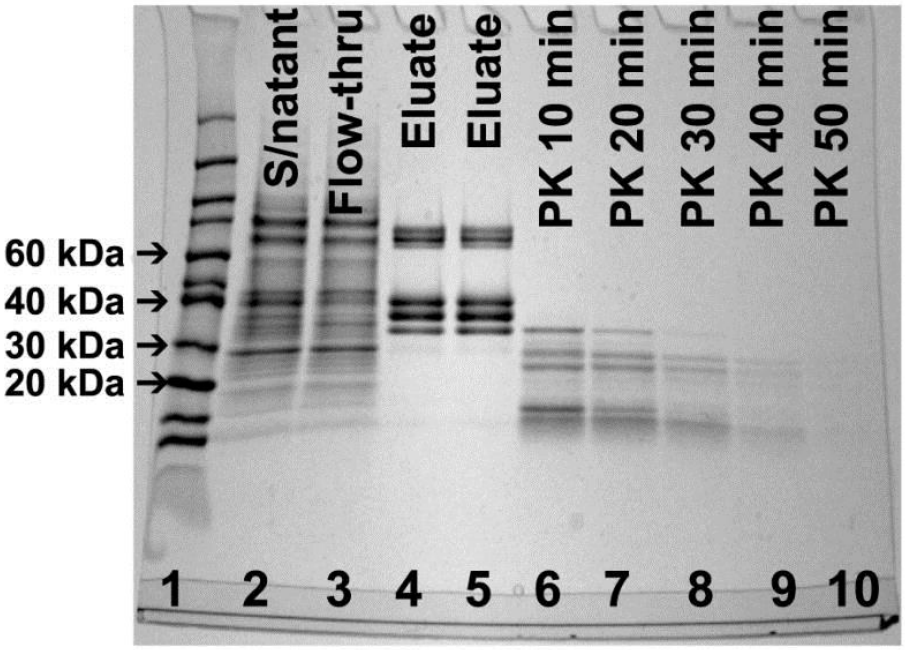

Figure 6: Sensitivity of VpAP:D99A to incubation with proteinase K, monitored by SDS-PAGE analysis. Supernatant of *E. coli* culture expressing ΔspΔCVpAP:D99A*$(His)_6$ (Lane 2) was applied to Co(II)-affinity resin. Non-binding material flowed through the column in the absence of imidazole (Lane 3). ΔspΔCVpAP:D99A*$(His)_6$ eluted with imidazole (Lanes 4 and 5) and was subsequently incubated with proteinase K for 10 - 50 min (Lanes 6 - 10).

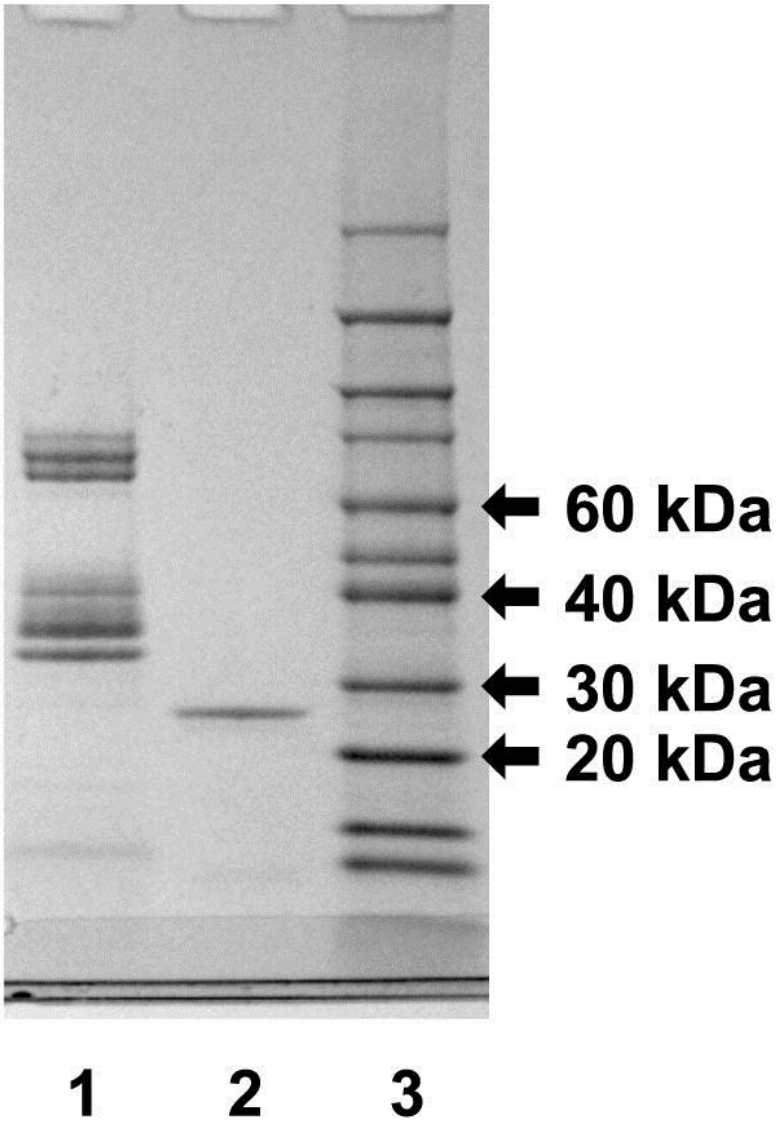

Figure 7: Autoprocessing of VpAP:D99M during extended dialysis monitored by SDS-PAGE analysis. Lane 1, ΔspΔCVpAP:D99A*$(His)_6$-containing fraction that eluted from Co(II)-affinity resin with imidazole; Lane 2, after 13 d dialysis against HEPES buffer at 4 °C; Lane 3, M_r markers.

The Cys223-Cys227 disulfide bond is also a key structural feature of the active site. It is perhaps possible that some active site local structure is preserved, even in the presence of SDS, in wild-type VpAP during SDS-PAGE; it is noteworthy that mass spectrometry has verified that purified, mature VpAP does not run on SDS-PAGE corresponding to its correct M_r [71]. The local structure may not be so preserved in VpAP:D99*X* variants, however; a hypersensitivity to PK

and heat treatment are consistent with lower structural stability. In that case, at least six bands may be expected on SDS-PAGE, three dimeric species with intermolecular disulfide bonds between the N-terminal propeptide cysteine of one monomer and three monomeric species with a single disulfide; note that the suspected proximity of the N-terminal propeptide to the active site, suggested by the inhibitory effect on activity, would facilitate intramolecular disulfide bond formation between the N-terminal propeptide and either of Cys223 or Cys227 if the Cys223-Cys227 disulfide bond itself were not subject to additional stabilization. Further work that is outside the scope of the current study is clearly necessary to fully understand the behavior of VpAP polypeptide constructs on SDS-PAGE. However, there is available information on (i) the Cys content of mature and unprocessed VpAP constructs, (ii) the thermostability and stable disulfide bond in mature wild-type VpAP, (iii) the structural relationship between D99, the active site, and the disulfide bond, (iv) the much lower structural stability of D99 mutants and (v) the anomalous behavior on SDS-PAGE of purified, mature VpAP of mass-spectrometry-verified M_r. These data are consistent with, and suggest a mechanism for, multiple bands on SDS-PAGE for unprocessed VpAP constructs, a single band for purified VpAP, and a different and more complex band profile for VpAP:D99*X* variants unprocessed polypeptide constructs than for wild-type.

Upon treatment with PK (Step B), VpAP:D99A was rapidly degraded. After 10 min, bands at 28, 30 and 32 kDa were observable on SDS-PAGE, along with fragments of lower apparent M_r (lane 6, Figure 6). After 30 – 40 min, however, these bands had disappeared (lanes 8 and 9, Figure 6), and, after 50 min, no protein at all was observable on the gel (lane 10, Figure 6).

The lengthy methods of either SDS-PAGE or measurement of very low levels of activity are, obviously, impractical for real-time determination of when to terminate Step B, and this procedure could not be reliably or reproducibly employed to process ΔspΔCVpAP:D99*X**$(His)_6$. Instead, the alternative procedure of extended dialysis *without* PK, Step E, was employed. VpAP:D99M displayed the same SDS-PAGE profile as VpAP:D99A, following Step A (lane 1, Figure 7), and a similar sensitivity to PK treatment. However, upon extended dialysis at 4 °C against HEPES buffer, the bands in the

Protein Expression and Purification, Vol. 66, No. 1 (July 2009): pg. 91-101. DOI.

range of apparent M_r = 30 − 40 kDa, and M_r ≈ 62 kDa, lost intensity and a band with apparent M_r ≈ 28 kDa emerged, corresponding to the 31 ± 1 kDa species characterized by mass spectrometry, until, after 13 d, only the band at M_r ≈ 28 kDa was observable (lane 2, Figure 7). The N-terminal amino acid sequence of this species was found to be TLASFVM, corresponding to the final six amino acids of the N-terminal propeptide, and the N-terminal methionine of mature VpAP; this confirmed that the N-terminus was autoprocessed during dialysis. Step D, a second application to Co(II)-affinity resin, was then carried out. SDS-PAGE analysis (Figure 8) clearly showed that VpAP:D99M isolated from Step E did not bind to the resin and that, therefore, the C-terminal region had also been removed during Step E. Circular dichroism spectropolarimetery of D99M yielded a spectrum indistinguishable from that of the "32 kDa" form of wild-type recombinant, fully active enzyme (Figure 9). If M_r for VpAP:D99M were really 28 kDa, this could only correspond to the loss of a large C-terminal α-helix, given the experimentally obtained N-terminal sequences, and the circular dichroism spectra would be expected to be significantly different.

Protein Expression and Purification, Vol. 66, No. 1 (July 2009): pg. 91-101. DOI.

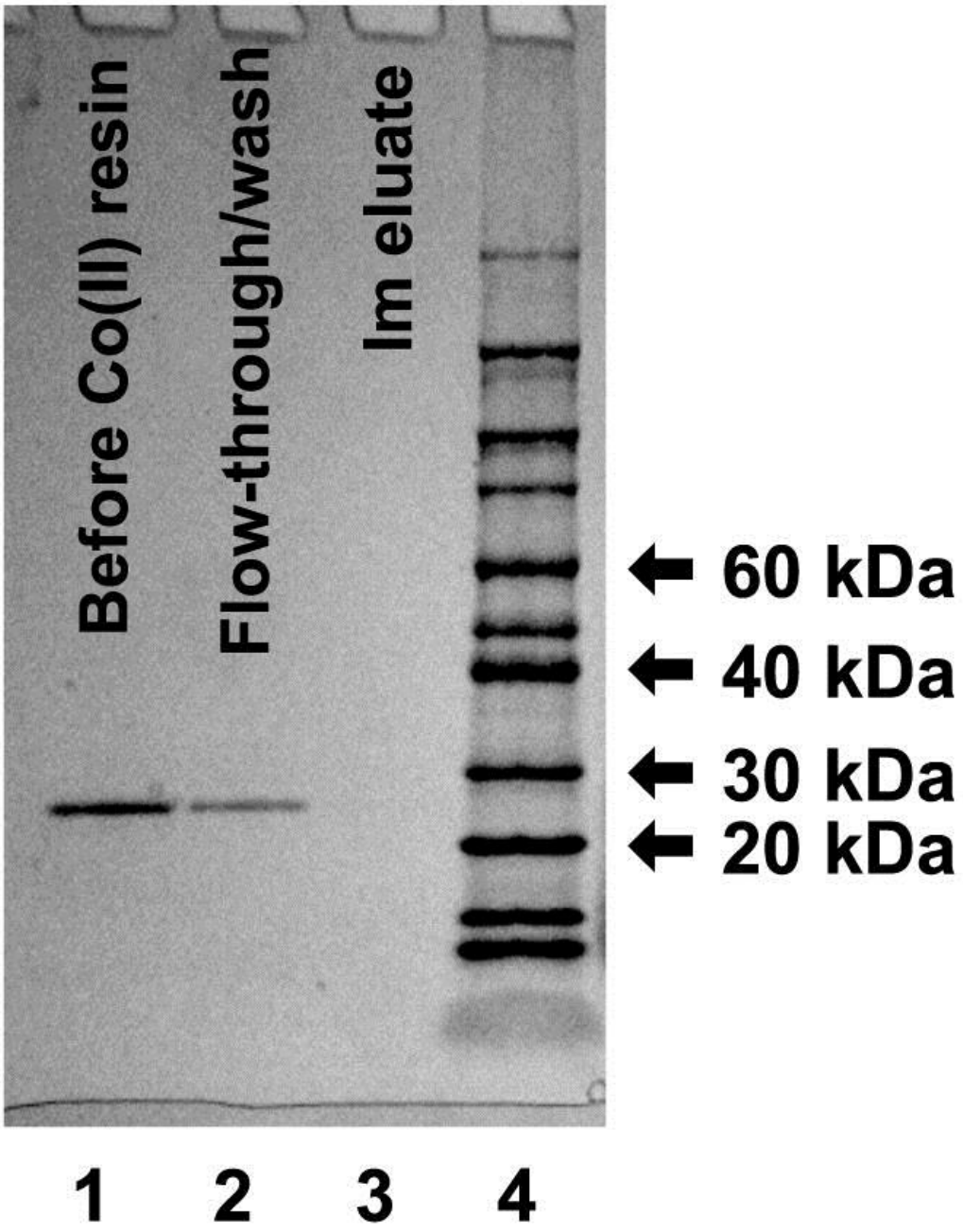

Figure 8: Loss of $(His)_6$ construct from VpAP:D99M. Lane 1, VpAP:D99M after extended dialysis; Lane 2, Flow-through from Co(II)-affinity resin during application of VpAP:D99M and washing with buffer; Lane 3, Eluate upon application of imidazole; Lane 4, M_r markers. Lane 1 corresponds to 1.2 µg protein and Lane 2 corresponds to 0.3 µg protein (10 µl of the sample described in Table 2, in each case).

Protein Expression and Purification, Vol. 66, No. 1 (July 2009): pg. 91-101. DOI.

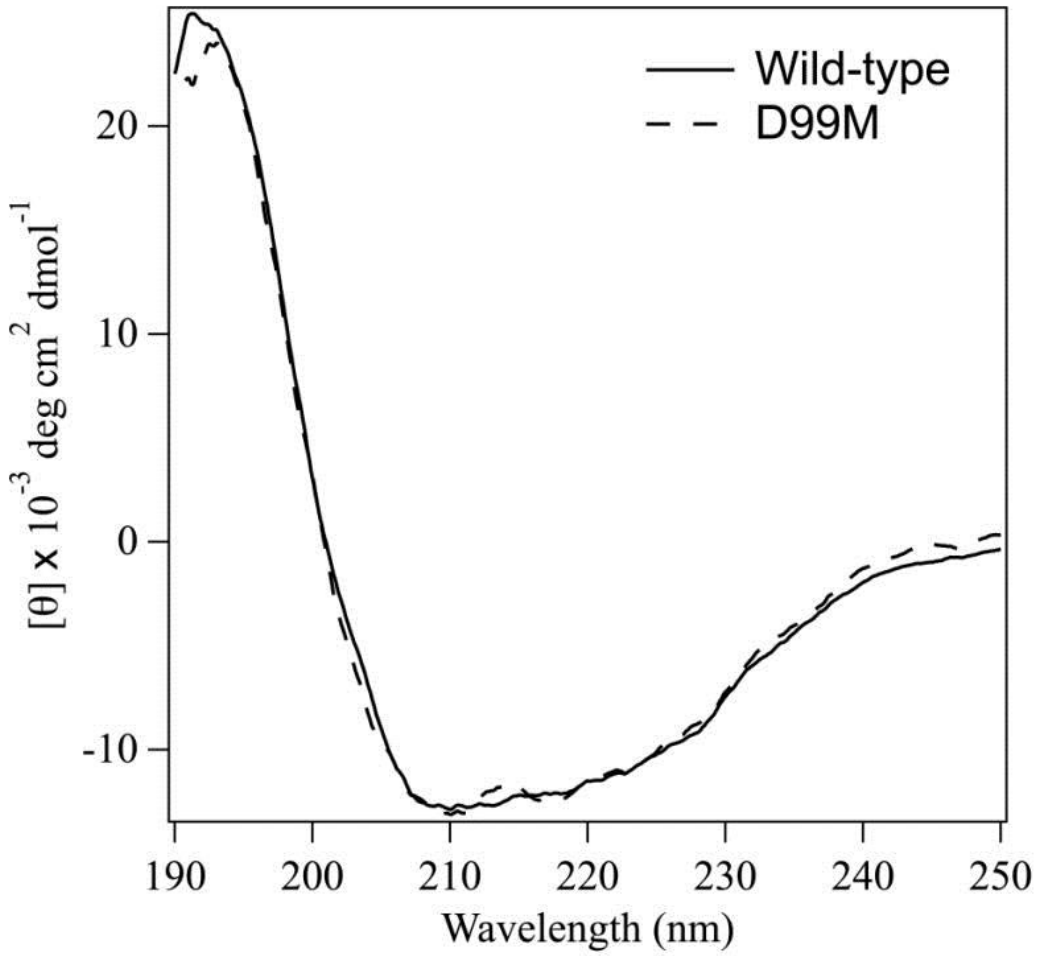

Figure 9: Circular dichroism spectra of recombinant wild-type VpAP (solid line) and VpAP:D99M (dashed line).

Crystallization and crystallography of wild-type VpAP

Wild type VpAP protein readily formed hexagonal crystals (Figure 10) with a space group of $P6_122$. The structure was determined to a resolution of 1.95 Å (1 Å = 0.1 nm; PDB code 3F4H) and the crystallographic data collection and refinement statistics are given in Table 3. The protein fold was essentially identical to those structures already published. For comparison, the present structure, 3F4H, and an earlier structure, 1LOK [38], were superimposable (LSQMAN) with a root mean square deviation of 0.120 Å in Cα position. The inter-Zn distances were 3.40 Å (3F4H) and 3.45 Å (1LOK). The crystal structure also provided information on the C-terminus of the fully processed protein. The residues comprising the sequence MGSATG were all

Protein Expression and Purification, Vol. 66, No. 1 (July 2009): pg. 91-101. DOI.

clearly identifiable from the electron density and, as with natively expressed VpAP, only the short C-terminal sequence DTPTPGNQ could not be inferred from X-ray diffraction. In addition, the pre-N-terminal residues ASFV were not clear from the X-ray diffraction data. The possible range of M_r for the crystallized recombinant VpAP is, then, 31,388 to 32,640 D (not including Zn).

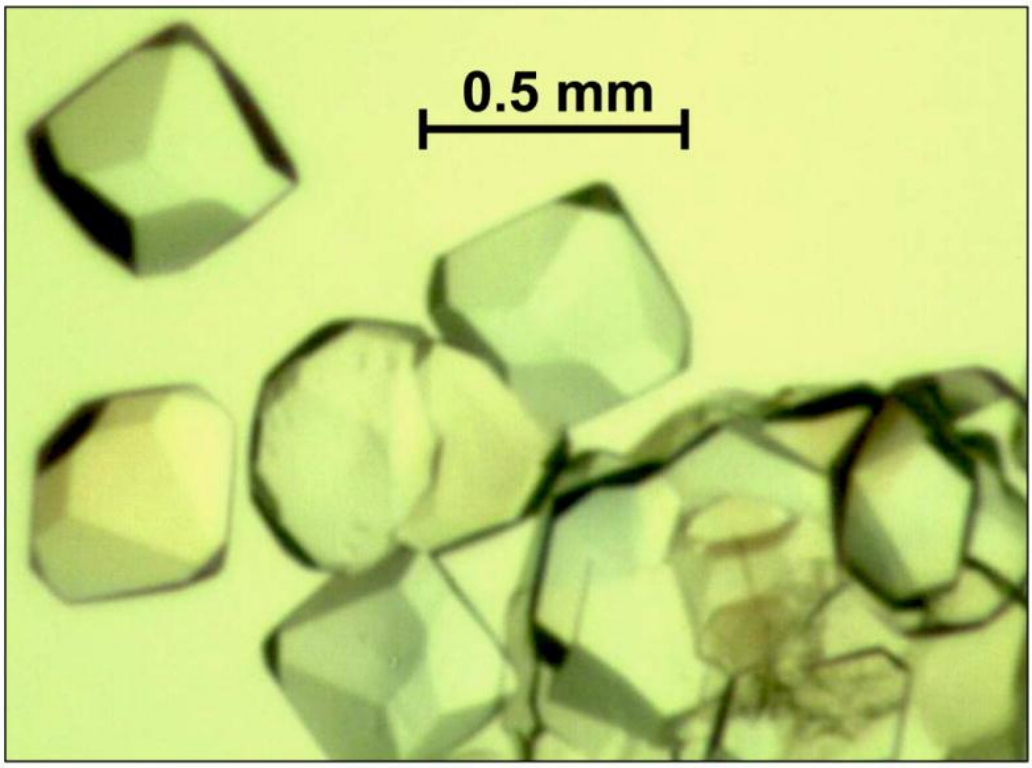

Figure 10: Crystals of heterologously expressed VpAP.

Table 3: Crystallographic data and refinement statistics for VpAP structure 3F4H

Data collection	
Resolution (Highest Resolution Shell) (Å)	50 - 1.95 (2.02 - 1.95)
Total Reflections	79269
Unique Reflections	23164
Completeness (%)	95.5 (97.7)
$\langle I/(\sigma I)\rangle$	11.6 (2.6)
Cell Dimensions	a = b = 108.4 Å, c = 93.5 Å; γ = 120°
Space Group	$P6_122$
R_{merge}	0.094 (0.420)

Protein Expression and Purification, Vol. 66, No. 1 (July 2009): pg. 91-101. DOI.

V_m, Solvent Content	2.48 Å^3 D^{-1}, 50.4 %
Monomers in Asymmetric Unit	1
Refinement	
Number of Protein Atoms	2236
Number of Water Molecules	150
Number of Bound Ligands	8
Number of Zn Atoms	2
Number of Na Atoms	2
$B_{av.}$ Main Chain (Å^2)	14.9
$B_{av.}$ Side Chain (Å^2)	15.6
$B_{av.}$ Zn (Å^2)	14.3
$B_{av.}$ Tris (Å^2)	19.6
$B_{av.}$ Na (Å^2)	11.1
$B_{av.}$ Water (Å^2)	17.7
$R_{cryst.}$ / R_{free}	0.191 / 0.229
R.M.S.D. Bond Length / Angle	0.009 Å / 1.138°
Ramachandran Plot	
Most Favored	88.4 %
Additional Favored	11.2 %
Generously Allowed	0.4 % (Met180)

Discussion

VpAP has been extensively studied, because of its high structural homology to many biomedically important metallohydrolases, and because of the actual and potential clinical utility of inhibitors of the enzyme [35, 36, 40]. In particular, the mechanism of action of the enzyme is seen as providing a prototypical template for the rational design of anti-cancer, anti-angiogenic and antibiotic chemotherapeutic agents. Despite much elegant work on the native wild-type enzyme, that has provided much insight into the catalytic mechanism, questions remain; even the roles of the distinct Zn(II) ions in the active site, once thought to be clear [60, 76, 97], are now somewhat controversial [39, 98]. The focus of recent structure-function research on VpAP, and on closely related enzymes, has been on site-directed variants [61-64, 98], as these may provide further insight into the structure-function relationships in VpAP.

Protein Expression and Purification, Vol. 66, No. 1 (July 2009): pg. 91-101. DOI.

A prerequisite to structure-function studies on site-directed variants of VpAP is a method by which these proteins can be expressed and purified. The challenges associated with heterologous expression and purification of VpAP are evident from earlier work, and have been particularly thoroughly addressed in a report by Bzymek, Holz and coworkers [71, 72]. Briefly, the problems include (i) the desirability of a mechanism by which VpAP is exported from the cell, to prevent inclusion body formation; (ii) the requirement for an N-terminal propeptide for correct folding; (iii) the inhibitory nature of the N-terminal propeptide, which makes identification and quantitation of unprocessed VpAP* by activity very difficult; (iv) anomalous behavior of VpAP* on SDS-PAGE gels; (v) the need for aggressive treatment with proteases and heat to process VpAP* to VpAP; (vi) multiple lengthy and inefficient chromatographic separations. Despite these challenges, Bzymek *et al.* were able to design a protocol for isolation of heterologously expressed VpAP that yielded wild-type and some site-directed variant forms of VpAP.

Despite the successes of the method of Bzymek, Holz and coworkers, two outstanding issues led us to revisit the expression and purification of VpAP from an *E. coli* expression system. The first was that we were unable to isolate some site-directed variants using this method. Where initial expression was low, the losses in terms of recoverable material during the traditional chromatographic steps were unacceptable. In addition, as our data clearly show, some variants were so sensitive to proteinase K treatment, and the procedure so difficult to control with variants exhibiting low specific activity, that incubation with proteinase K could not be reliably used to cleave the N-terminal propeptide. The second outstanding issue was that of final purity of the product. Many site-directed variants of interest in structure-function studies have very low activities compared to wild-type VpAP. Reported activities of *e.g.* 0.004 % of that of wild-type have been reported [61]. Important mechanistic information is available from kinetic studies of variants with even very low activities; for instance, K'_m informs on the ability of a kinetically compromised variant to form a Michealis complex with substrate. However, these studies rely on the level of contamination by other proteolytic enzymes being extremely low, much lower than can be determined by SDS-PAGE. While heat treatment may be expected to denature most proteins other than VpAP, there is no analytical way to determine that

heat treatment does indeed destroy all contaminating proteases to a remaining level of ≪ 0.004 %. In addition, some VpAP site-directed variants are unstable toward heat treatment as well as toward proteinase K.

The expression of VpAP as a construct with a $(His)_6$ adduct facilitated a very rapid and effective first purification step. Three bands were evident on SDS-PAGE after this first step; two of the bands were shown to be due to ΔspΔCVpAP*$(His)_6$, indicating anomalous behavior on SDS. Given (i) the known propensity of both unprocessed and processed VpAP to behave anomalously on SDS-PAGE, (ii) the requirement of imidazole for elution of the unprocessed material from the Co(II)-affinity resin, (iii) a constant ratio of the intensities of the three bands among fractions from the Co(II)-affinity column, and (iv) that a single product resulted from processing of the unprocessed material, it is likely that all three bands were due to ΔspΔCVpAP*$(His)_6$. Earlier attempts to employ a "ΔC" construct, *i.e.* one lacking 43 amino acids of the C-terminal propeptide ("pET27b(+)-43AAP"), resulted in a processed product with only 35 % of the activity of the native enzyme [71]. In contrast, processing of ΔspΔCVpAP*$(His)_6$, in which the entire C-terminal propeptide was deleted, provided VpAP with activity as high as any reported and with K'_m in the range of typically reported values.

The use of a $(His)_6$-containing construct allowed for rapid purification of VpAP but presented the concern that the $(His)_6$ construct may not be removed during processing. As VpAP is a transition ion-dependent enzyme, structure-function studies addressing the active site would be compromised by binding of metal ions to the $(His)_6$ sequence. In particular, Co(II) is commonly used as a spectroscopically active substitute for the native Zn(II) but $(His)_6$ has a relatively high affinity for Co(II). An important final step, therefore, was the reapplication of fully processed VpAP to TALON Co(II)-affinity resin, and only fractions that *did not* bind, under the conditions that ΔspΔCVpAP*$(His)_6$*does* bind, were retained. In practice, no SDS-PAGE-detectable material was actually observed in fractions collected upon subsequent application of imidazole, indicating highly efficient cleavage. The specific site of cleavage is unclear, but the crystal structure of wild-type VpAP indicated that it is somewhere in the short C-terminal sequence DTPTPGNQLE that immediately

Protein Expression and Purification, Vol. 66, No. 1 (July 2009): pg. 91-101. DOI.

precedes $(His)_6$. The ready crystallization, and sub-2 Å X-ray diffraction of the crystals, suggests a highly pure and homogeneous final product.

The use of the $(His)_6$ construct was also applied to VpAP variants. One of the principal advantages was the rapid separation of fragile variants, such as the VpAP:D99*X* family, from other proteolytic enzymes. Studies with PK have shown these variants to be far less resistant than wild-type VpAP to proteolytic action, and the one-step Co(II)-affinity column isolation of ΔspΔCVpAP*:D99*X*$(His)_6$ has replaced much lengthier and less effective hydrophobic interaction and anion exchange chromatographic steps that have been traditionally employed. Key to the use of ΔspΔCVpAP*:D99*X*$(His)_6$, however, was the observation that solutions that had undergone exhaustive dialysis, followed by filtration, did not bind to Co(II)-affinity resin when reapplied. This observation suggested that ΔspΔCVpAP*:D99*X*$(His)_6$ was capable of autoprocessing. Along with a role for a neutral protease expressed by *V. proteolyticus* in processing VpAP*, autoprocessing by VpAP has also long been suspected. However, as crude preparations have not been free of other proteolytic activity, it has been difficult to confirm such a role. In the case of the ΔspΔCVpAP*:D99*X*$(His)_6$ variants, however, Co(II)-affinity resin chromatography provided a highly purified species, notwithstanding the anomalous behavior on SDS-PAGE. In addition to removal of the $(His)_6$ adduct, exhaustive dialysis was shown by SDS-PAGE, and earlier mass spectrometry studies on wild-type VpAP, to have processed ΔspΔCVpAP*:D99*X*$(His)_6$ to a single species with M_r = 31 kDa. This indicated removal of the N-terminal propeptide, and this was confirmed by N-terminal sequencing. It was confirmed by circular dichroism spectropolarimetry that extensive C-terminal processing did *not* occur, despite the apparent M_r of 28 kDa from SDS-PAGE. The 3 - 4 kDa C-terminal region that would have been lost from the 32 kDa protein to form a 28 kDa species would consist almost entirely of α-helix, and the circular dichroism spectrum would have differed significantly from that of wild-type in the 200 - 240 nm region.

In conclusion, we have developed protocols for purification of wild-type VpAP, and of protease-intolerant site-directed variants. The replacement of a C-terminal propeptide with a $(His)_6$ adduct facilitates very rapid isolation of the expressed polypeptide from contaminating

Protein Expression and Purification, Vol. 66, No. 1 (July 2009): pg. 91-101. DOI.

proteolytic activity, from the supernatant of cultures of *E. coli*. Post-translational processing of the purified polypeptide to the mature, functional enzyme can be effected by traditional exposure to heat or proteolytic activity or, for protease-intolerant variants, by an apparently autocatalytic mechanism. Isolation of a final product that is demonstrably devoid of the $(His)_6$ construct is possible by a repeat application to Co(II)-affinity resin. This advance will facilitate the isolation and study of site-directed variants of VpAP with structure-function relationship interest.

Acknowledgments

The authors would like to thank Wei Yong and Prof. Jung-Ja Kim, Department of Biochemistry, Medical College of Wisconsin, for invaluable assistance with crystallography. This work was supported by the National Institutes of Health (NIAID R01 AI056231 to B.B.).

Abbreviations used

ΔspVpAP*(His)$_6$ heterologously expressed *V. proteolyticus* aminopeptidase polypeptide containing the N- and C-terminal propeptides, the mature enzyme region, and a C-terminal $(His)_6$ construct, but lacking a 23 amino acid N-terminal signal sequence

ΔspΔCVpAP*(His)$_6$ heterologously expressed *V. proteolyticus* aminopeptidase polypeptide containing the N-terminal propeptide, the mature enzyme region, and a C-terminal $(His)_6$ construct, but lacking a 23 amino acid N-terminal signal sequence and the C-terminal propeptide

HEPES *N*-(2-hydroxyethyl)-piperazine-*N*′-2-ethanesulfonic acid

IPTG isopropyl *β*-D-1-thiogalactopyranoside

LB Lysogeny broth (Luria-Bertani)

LPNA L-leucine-*p*-nitroanilide

mAP metalloaminopeptidase

M$_r$ relative molecular mass

PK proteinase K from *Tritirachium album*

PSMA prostate-specific membrane antigen

VpAP *Vibrio proteolyticus* leucine aminopeptidase (32 kDa mature form)

VpAP* *Vibrio proteolyticus* leucine aminopeptidase (54 kDa proenzyme)

citable form. Please note that during the production process errors may be discovered which could affect the content, and all legal disclaimers that apply to the journal pertain.

References

1. Bradshaw RA. Protein translocation and turnover in eukaryotic cells. Trends Biochem Sci. 1989;14:276–279.
2. Meinnel T, Mechulam Y, Blanquet S. Methionine as translation start signal: a review of the enzymes of the pathway in *Escherichia coli*. Biochimie. 1993;75:1061–1075.
3. Arfin SM, Bradshaw RA. Cotranslational processing and protein turnover in eukaryotic cells. Biochemistry. 1988;27:7979–7984.
4. Bachmair A, Finley D, Varshavsky A. In vivo half-life of a protein is a function of its amino-terminal residue. Science. 1986;234:179–186.
5. Arechaga G, Martinez JM, Prieto I, Ramirez MJ, Alba F, Ramirez M. Changes in membrane-bound leucine aminopeptidase activity during maturation and ageing of brain. Biochem Molec Biol Int. 1999;47:851–856.
6. Babst R, Bongiorno L, Marini M, Marzano M, Spagnoli G, Roda LG, Urbani A. Age-induced increase of leucine enkephalin enzyme degradation in human plasma. Peptides. 1998;19:1155–1163.
7. Martinez JM, Prieto I, Ramirez MJ, de Gasparo M, Hermoso F, Arias JM, Alba F, Ramirez M. Sex differences and age-related changes in human serum aminopeptidase A activity. Clinica Chim Acta. 1998;274:53–61.
8. Mathe G. Bestatin, an aminopeptidase inhibitor with a multi-pharmacological function. Biomed Parmacother. 1991;45:49–54.
9. Ramirez M, Arechaga G, Sanchez B, Ozaita A, Lardelli P. Developmental and ageing changes in aminopeptidase activities in selected tissues of the rat. Experientia. 1993;49:300–303.
10. Salminen A, Vihko V. Effects of age and prolonged running on proteolytic capacity in mouse cardiac and skeletal muscles. Acta Physiol Scand. 1981;112:89–95.
11. Betz P. Histological and enzyme histochemical parameters for the age estimation of human skin wounds. Int J Legal Med. 1994;107:60–68.
12. Duranton B, Schleiffer R, Gosse F, Raul F. Preventive administration of ornithine alpha-ketoglutarate improves intestinal mucosal repair after transient ischemia in rats. Criti Care Med. 1998;26:120–125.
13. Prager MD, Sabeh F, Baxter CR, Atiles L, Hartline B. Dipeptidyl peptidase IV and aminopeptidase in burn wound exudates: implications for wound healing. J Trauma. 1994;36:629–633.
14. Spector GJ. The role of aminopeptidases in inflammatory and neoplastic tissues. Laryngoscope. 1976;86:1218–1240.

15. Spector GJ. Leucine and alanine aminopeptidase activities in experimentally induced intradermal granulomas and late stages of wound healing in the rat. Lab Invest. 1977;36:1–7.
16. Blondin J, Taylor A. Measures of leucine aminopeptidase can be used to anticipate UV-induced age-related damage to lens proteins: ascorbate can delay this damage. Mech Ageing Dev. 1987;41:39–46.
17. Fukui HN, Merola LO, Kinoshita JH. A possible cataractogenic factor in the Nakano mouse lens. Exp Eye Res. 1978;26:477–485.
18. Sharma KK, Ortwerth BJ. Aminopeptidase III activity in normal and cataractous lenses. Curr Eye Res. 1986;5:373–380.
19. Swanson AA, Davis RM, McDonald JK. Dipeptidyl peptidase III of human cataractous lenses. Partial purification. Curr Eye Res. 1984;3:287–291.
20. Swanson AA, Davis RM, Meinhardt NC, Kuck KD, Kuck JF., Jr Proteases in the Emory mouse cataract. Invest Opthalmol Vis Sci. 1985;26:1035–1037.
21. Taylor A, Daims M, Lee J, Surgenor T. Identification and quantification of leucine aminopeptidase in aged normal and cataractous human lenses and ability of bovine lens LAP to cleave bovine crystallins. Curr Eye Res. 1982;2:47–56.
22. Velasco PT, Lukas TJ, Murthy SN, Duglas-Tabor Y, Garland DL, Lorand L. Hierarchy of lens proteins requiring protection against heat-induced precipitation by the alpha crystallin chaperone. Exp Eye Res. 1997;65:497–505.
23. Gutheil WG, Subramanyam M, Flentke GR, Sanford DG, Munoz E, Huber BT, Bachovchin WW. Human immunodeficiency virus 1 Tat binds to dipeptidyl aminopeptidase IV (CD26): a possible mechanism for Tat's immunosuppressive activity. Proc Natl Acad Sci USA. 1994;91:6594–6598.
24. Pulido-Cejudo G, Conway B, Proulx P, Brown R, Izaguirre CA. Bestatin-mediated inhibition of leucine aminopeptidase may hinder HIV infection. Antivir Res. 1997;36:167–177.
25. Schols D, Proost P, Struyf S, Wuyts A, De Meester I, Scharpe S, Van Damme J, De Clercq E. CD26-processed RANTES(3-68), but not intact RANTES, has potent anti-HIV-1 activity. Antivir Res. 1998;39:175–187.
26. Su SF, Amidon GL. Investigation into the intestinal metabolism of [D-Ala1] peptide T amide: implication for oral drug delivery. Biochim Biophys Acta. 1995;1245:62–68.
27. Hashida H, Takabayashi A, Kanai M, Adachi M, Kondo K, Kohno N, Yamaoka Y, Miyake M. Aminopeptidase N is involved in cell motility and angiogenesis: its clinical significance in human colon cancer. Gastroenterol. 2002;122:376–386.

28. Lowther WT, Matthews BW. Structure and function of the methionine aminopeptidases. Biochim Biophys Acta. 2000;1477:157–167.
29. Pasqualini R, Koivunen E, Kain R, Lahdenranta J, Sakamoto M, Stryhn A, Ashmun RA, Shapiro LH, Arap W, Ruoslahti E. Aminopeptidase N is a receptor for tumor-homing peptides and a target for inhibiting angiogenesis. Cancer Res. 2000;60:722–727.
30. Seli E, Senturk LM, Bahtiyar OM, Kayisli UA, Arici A. Expression of aminopeptidase N in human endometrium and regulation of its activity by estrogen. Fertil Steril. 2001;75:1172–1176.
31. Zhang P, Nicholson DE, Bujnicki JM, Su X, Brendle JJ, Ferdig M, Kyle DE, Milhous WK, Chiang PK. Angiogenesis inhibitors specific for methionine aminopeptidase 2 as drugs for malaria and leishmaniasis. J Biomed Sci. 2002;9:34–40.
32. Essler M, Ruoslahti E. Molecular specialization of breast vasculature: a breast-homing phage-displayed peptide binds to aminopeptidase P in breast vasculature. Proc Natl Acad Sci USA. 2002;99:2252–2257.
33. Gorrell MD, Gysbers V, McCaughan GW. CD26: a multifunctional integral membrane and secreted protein of activated lymphocytes. Scand J Immunol. 2001;54:249–264.
34. Ishii K, Usui S, Sugimura Y, Yoshida S, Hioki T, Tatematsu M, Yamamoto H, Hirano K. Aminopeptidase N regulated by zinc in human prostate participates in tumor cell invasion. Int J Cancer. 2001;92:49–54.
35. Holz RC, Bzymek KP, Swierczek SI. Co-catalytic metallopeptidases as pharmaceutical targets. Curr Opin Chem Biol. 2003;7:197–206.
36. Bennett B. EPR of Co(II) as a structural and mechanistic probe of metalloprotein active sites: characterisation of an aminopeptidase. Curr Topics Biophys. 2002;26:49–57.
37. Desmarais W, Bienvenue DL, Bzymek KP, Petsko GA, Ringe D, Holz RC. The high-resolution structures of the neutral and the low pH crystals of aminopeptidase from *Aeromonas proteolytica*. J Biol Inorg Chem. 2006;11:398–408.
38. Desmarais WT, Bienvenue DL, Bzymek KP, Holz RC, Petsko GA, Ringe D. The 1.20 A resolution crystal structure of the aminopeptidase from *Aeromonas proteolytica* complexed with Tris: a tale of buffer inhibition. Structure. 2002;10:1063–1072.
39. Kumar A, Periyannan GR, Narayanan B, Kittell AW, Kim JJ, Bennett B. Experimental evidence for a metallohydrolase mechanism in which the nucleophile is not delivered by a metal ion: EPR spectrokinetic and structural studies of aminopeptidase from *Vibrio proteolyticus*. Biochem J. 2007;403:527–536.
40. Stamper CC, Bienvenue DL, Bennett B, Ringe D, Petsko GA, Holz RC. Spectroscopic and X-ray crystallographic characterization of bestatin

bound to the aminopeptidase from *Aeromonas (Vibrio) proteolytica*. Biochemistry. 2004;43:9620–9628.
41. Stamper C, Bennett B, Edwards T, Holz RC, Ringe D, Petsko G. Inhibition of the aminopeptidase from *Aeromonas proteolytica* by L-leucinephosphonic acid. Spectroscopic and crystallographic characterization of the transition state of peptide hydrolysis. Biochemistry. 2001;40:7035–7046.
42. Burley SK, David PR, Sweet RM, Taylor A, Lipscomb WN. Structure determination and refinement of bovine lens leucine aminopeptidase and its complex with bestatin. J Mol Biol. 1992;224:113–140.
43. Centres for Disease Control and Prevention. *Aeromonas* Wound Infections Associated with Outdoor Activities: California. Morb Mortal Wkly Rep. 1990;39:334–335.
44. Centres for Disease Control and Prevention. Outbreak of *Vibrio parahaemolyticus* infection associated with eating raw oysters and clams harvested from Long Island Sound: Connecticut, New Jersey and New York, 1998. Morb Mortal Wkly Rep. 1999;48:48–51.
45. Liu S, Widom J, Kemp CW, Crews CM, Clardy J. Structure of human methionine aminopeptidase-2 complexes with fumagillin. Science. 1998;282:1324–1327.
46. Maras B, Greenblatt HM, Shoham G, Spungin-Bialik A, Blumberg S, Barra D. Aminopeptidase from *Streptomyces griseus*: primary structure and comparison with other zinc-containing aminopeptidases. Eur J Biochem. 1996;236:843.
47. Sin N, Meng L, Wang MQ, Wen JJ, Bornmann WG, Crews CM. The anti-angiogenic agent fumagillin covalently binds and inhibits the methionine aminopeptidase, MetAP-2. Proc Natl Acad Sci USA. 1997;94:6099–6103.
48. Toma C, Honma Y. Cloning and genetic analysis of the *Vibrio cholerae* aminopeptidase gene. Infect Immun. 1996;64:4495–4500.
49. Mahadevan D, Saldanha JW. The extracellular regions of PSMA and the transferrin receptor contain an aminopeptidase domain: implications for drug design. Protein Sci. 1999;8:2546–2549.
50. Horoszewicz JS, Kawinski E, Murphy GP. Monoclonal antibodies to a new antigenic marker in epithelial prostatic cells and serum of prostatic cancer patients. Anticancer Res. 1987;7:927–935.
51. Curnis F, Arrigoni G, Sacchi A, Fischetti L, Arap W, Pasqualini R, Corti A. Differential binding of drugs containing the NGR motif to CD13 isoforms in tumor vessels, epithelia, and myeloid cells. Cancer Res. 2002;62:867–874.
52. Griffith EC, Su Z, Niwayama S, Ramsay CA, Chang YH, Liu JO. Molecular recognition of angiogenesis inhibitors fumagillin and ovalicin by

methionine aminopeptidase 2. Proc Natl Acad Sci USA. 1998;95:15183–15188.
53. Griffith EC, Su Z, Turk BE, Chen S, Chang YH, Wu Z, Biemann K, Liu JO. Methionine aminopeptidase (type 2) is the common target for angiogenesis inhibitors AGM-1470 and ovalicin. Chem Biol. 1997;4:461–471.
54. Lowther WT, McMillen DA, Orville AM, Matthews BW. The anti-angiogenic agent fumagillin covalently modifies a conserved active-site histidine in the *Escherichia coli* methionine aminopeptidase. Proc Natl Acad Sci USA. 1998;95:12153–12157.
55. Niimoto M, Hattori T. Prospective randomized controlled study on bestatin in resectable gastric cancer. Biomed Pharmacother. 1991;45:121–124.
56. Sakuraya M, Tamura J, Itoh K, Kubota K, Naruse T. Aminopeptidase inhibitor ubenimex inhibits the growth of leukaemic cell lines and myeloma cells through its cytotoxicity. J Int Med Res. 2000;28:214–221.
57. Shibuya K, Chiba S, Hino M, Kitamura T, Miyagawa K, Takaku F, Miyazano K. Enhancing effect of ubenimex (bestatin) on proliferation and differentiation of hematopoietic progenitor cells, and the suppressive effect on proliferation of leukemic cell lines via peptidase regulation. Biomed Pharmacother. 1991;45:71–80.
58. Taunton J. How to starve a tumor. Chem Biol. 1997;4:493–496.
59. Vaughan MD, Sampson PB, Honek JF. Methionine in and out of proteins: targets for drug design. Curr Med Chem. 2002;9:385–409.
60. DePaola C, Bennett B, Holz RC, Ringe D, Petsko G. L-Butaneboronic acid binding to *Aeromonas proteolytica* aminopeptidase: a case of arrested development. Biochemistry. 1999;38:9048–9053.
61. Bzymek KP, Holz RC. The catalytic role of glutamate 151 in the leucine aminopeptidase from *Aeromonas proteolytica*. J Biol Chem. 2004;279:31018–31025.
62. Bzymek KP, Moulin A, Swierczek SI, Ringe D, Petsko GA, Bennett B, Holz RC. Kinetic, spectroscopic, and X-ray crystallographic characterization of the functional E151H aminopeptidase from *Aeromonas proteolytica*. Biochemistry. 2005;44:12030–12040.
63. Bzymek KP, Swierczek SI, Bennett B, Holz RC. Spectroscopic and thermodynamic characterization of the E151D and E151A altered leucine aminopeptidases from *Aeromonas proteolytica*. Inorg Chem. 2005;44:8574–8580.
64. Davis RM, Bienvenue DL, Swierczek SI, Gilner D, Rajagopal L, Bennett B, Holz RC. Kinetic and spectroscopic characterization of the E134A- and E134D-altered dapE-encoded N-succinyl-L,L-diaminopimelic acid desuccinylase from *Haemophilus influenzae*. J Biol Inorg Chem. 2006;11:206–216.

65. Merkel JR, Traganza ED. Possible symbiotic role of proteolytic and cellulolytic bacteria found in the digestive system of a marine isopod. Bact Proc. 1958:53–54.
66. Prescott JM, Wilkes SH. *Aeromonas aminopeptidase*: purification and some general properties. Arch Biochem Biophys. 1966;117:328–336.
67. Prescott JM, Wilkes SH. Aeromonas aminopeptidase. Methods Enzymol. 1976;45:530–543.
68. Schalk C, Remy JM, Chevrier B, Moras D, Tarnus C. Rapid purification of the *Aeromonas proteolytica* aminopeptidase: crystallization and preliminary X-ray data. Arch Biochem Biophys. 1992;294:91–97.
69. Van Heeke G, Denslow S, Watkins JR, Wilson KJ, Wagner FW. Cloning and nucleotide sequence of the *Vibrio proteolyticus* aminopeptidase gene. Biochim Biophys Acta. 1992;1131:337–340.
70. Guenet C, Lepage P, Harris BA. Isolation of the leucine aminopeptidase gene from *Aeromonas proteolytica*. Evidence for an enzyme precursor. J Biol Chem. 1992;267:8390–8395.
71. Bzymek KP, D'Souza VM, Chen G, Campbell H, Mitchell A, Holz RC. Function of the signal peptide and N- and C-terminal propeptides in the leucine aminopeptidase from *Aeromonas proteolytica*. Prot Expr Purif. 2004;37:294–305.
72. Zhang ZZ, Nirasawa S, Nakajima Y, Yoshida M, Hayashi K. Function of the N-terminal propeptide of an aminopeptidase from *Vibrio proteolyticus*. Biochem J. 2000;350(Pt 3):671–676.
73. Prescott JM, Wilkes SH, Wagner FW, Wilson KJ. *Aeromonas* aminopeptidase. Improved isolation and some physical properties. J Biol Chem. 1971;246:1756–1764.
74. Nirasawa S, Nakajima Y, Zhang ZZ, Yoshida M, Hayashi K. Intramolecular chaperone and inhibitor activities of a propeptide from a bacterial zinc aminopeptidase. Biochem J. 1999;341(Pt 1):25–31.
75. Prescott JM, Wilkes SH. *Aeromonas* neutral protease. Methods Enzymol. 1976;45:404–415.
76. Bennett B, Holz RC. EPR studies on the mono- and dicobalt(II)-substituted forms of the aminopeptidase from *Aeromonas proteolytica*. Insight into the catalytic mechanism of dinuclear hydrolases. J Am Chem Soc. 1997;119:1923–1933.
77. Izawa N, Ishikawa S, Tanokura T, Ohta K, Hayashi K. Purification and characterization of *Aeromonas caviae* aminopeptidase possessing debittering activity. J Agric Food Chem. 1997;45:4897–4902.
78. Tang B, Nirasawa S, Kitaoka M, Hayashi K. The role of the N-terminal propeptide of the pro-aminopeptidase processing protease: refolding, processing, and enzyme inhibition. Biochem Biophys Res Commun. 2002;296:78–84.

79. Tang B, Nirasawa S, Kitaoka M, Hayashi K. In vitro stepwise autoprocessing of the proform of pro-aminopeptidase processing protease from *Aeromonas caviae* T-64. Biochim Biophys Acta. 2002;1596:16–27.
80. Baker JO, Wilkes SH, Bayliss ME, Prescott JM. Hydroxamates and aliphatic boronic acids: marker inhibitors for aminopeptidase. Biochemistry. 1983;22:2098–2103.
81. Tuppy H, Wiesbauer U, Wintesberger E. [Aminosäure-p-nitroanilide als substrate für aminopeptidäsen und andere proteolytische fermente]. Amino acid-p-nitroanilide as a substrate for aminopeptidases and other proteolytic enzymes. Hoppe Seylers Z Physiol Chem. 1962;329:278–288.
82. Marangoni AG. Enzyme Kinetics: A Modern Approach. John Wiley & Sons, Inc.; Hoboken, New Jersey: 2003. Characterization of enzyme activity; pp. 44–60.
83. Edelhoch H. Spectroscopic determination of tryptophan and tyrosine in proteins. Biochemistry. 1967;6:1948–1954.
84. Gill SC, von Hippel PH. Calculation of protein extinction coefficients from amino acid sequence data. Anal Biochem. 1989;182:319–326.
85. Gill SC, von Hippel PH. Calculation of protein extinction coefficients from amino acid sequence data. Anal Biochem. 1990;189:283. Erratum.
86. Rigaku. CrystalClear: An Integrated Program for the Collection and Processing of Area Detector Data. CrystalClear; Tokyo, Japan: 19972002.
87. Otwinowski Z, Minor W. Processing of X-ray diffraction data collected in oscillation mode. Methods Enzymol. 1997;276:307–326.
88. Kumar A, Periyannan GR, Narayanan B, Kittell AW, Kim JJ, Bennett B. Experimental evidence for a metallohydrolase mechanism in which the nucleophile is not delivered by a metal ion: EPR spectrokinetic and structural studies of aminopeptidase from *Vibrio proteolyticus*. Biochem J. 2007;403:527–536.
89. McCoy AJ, Grosse-Kunstleve RW, Adams PD, Winn MD, Storoni LC, Read RJ. Phaser crystallographic software. J Appl Crystallogr. 2007;40:658–674.
90. Emsley P, Cowtan K. Coot: model-building tools for molecular graphics. Acta Crystallogr. 2004;60:2126–2132.
91. Murshudov GN, Vagin AA, Dodson EJ. Refinement of macromolecular structures by the maximum-likelihood method. Acta Crystallogr. 1997;53:240–255.
92. N. Collaborative Computational Project. The CCP4 suite: programs for protein crystallography. Acta Crystallogr. 1994;Sect. D 50:760–763.

93. Laskowski RA, MacArthur MW, Moss DS, Thornton JM. Procheck: a program to check the stereochemical quality of protein structures. J Appl Crystallogr. 1993;26:283–291.
94. Niino YS, Chakraborty S, Brown BJ, Massey V. A New Old Yellow Enzyme of *Saccharomyces cerevisiae*. J Biol Chem. 1995;270:1983–1991.
95. Noel D, Nikaido K, Ames GF. A single amino acid substitution in a histidine-transport protein drastically alters its mobility in sodium dodecyl sulfate-polyacrylamide gel electrophoresis. Biochemistry. 1979;18:4159–4165.
96. Ustynyuk L, Bennett B, Edwards T, Holz RC. Inhibition of the aminopeptidase from *Aeromonas proteolytica* by aliphatic alcohols. Characterization of the hydrophobic substrate recognition site. Biochemistry. 1999;38:11433–11439.
97. Prescott JM, Wagner FW, Holmquist B, Vallee BL. Spectral and kinetic studies of metal-substituted *Aeromonas aminopeptidase*: nonidentical, interacting metal-binding sites. Biochemistry. 1985;24:5350–5356.
98. Ataie NJ, Hoang QQ, Zahniser MP, Tu Y, Milne A, Petsko GA, Ringe D. Zinc coordination geometry and ligand binding affinity: the structural and kinetic analysis of the second-shell serine 228 residue and the methionine 180 residue of the aminopeptidase from *Vibrio proteolyticus*. Biochemistry. 2008;47:7673–7683.